


A. CAMPOSEO^{1,*},
O.M. MARAGÒ²
B. FAZIO²
B. KLÖTER³
D. MESCHEDE³
U. RASBACH³
C. WEBER³
E. ARIMONDO¹

Resist-assisted atom lithography with group III elements

¹ CNR-INFM, Dipartimento di Fisica E. Fermi, Università di Pisa, Via F. Buonarroti 2, 56127 Pisa, Italy

² CNR-Istituto per i Processi Chimico-Fisici sez. Messina, via La Farina 237, 98123 Messina, Italy

³ Institut für Angewandte Physik der Universität Bonn, Wegelerstr. 8, 53115 Bonn, Germany

Received: 30 August 2006

Published online: 28 October 2006 • © Springer-Verlag 2006

ABSTRACT Resist-assisted atom lithography with group III elements, specifically with gallium and indium, is demonstrated. Self-assembled monolayers (SAM) of nonanethiols prepared on thin sputtered gold films were exposed to a beam of neutral gallium and indium atoms through a physical mask. The interaction of the Ga and In atoms with the nonanethiol layer, followed by a wet etching process, creates well defined structures on the gold film, with features below 100 nm. The threshold of the lithographic process was estimated by optical methods and found to be around 3 gallium atoms and 12 indium atoms per thiol molecule. Our experiments suggest that resist-assisted atom lithography can be realized with group III elements and possibly extended to new neutral atomic species.

PACS 07.77.Gx; 42.82.Cr; 81.16.Ta

1 Introduction

Atom lithography has attracted much interest in the past decade for its potential as a novel atomic nanofabrication (ANF) technique [1, 2]. Advantageous aspects of the method include parallel applications to a relatively large area, negligible contribution of atomic diffraction to the minimal feature size because of the small de Broglie wavelength of the atoms, and the low energy impact of the particles deposited on a substrate.

Both mechanical and optical masks can be used to modulate the atomic beam density transferred to a substrate for structure generation. Specifically, optical masks create periodic potentials that spatially segregate the atoms into an array of linear nanostructures spaced by a fraction of the laser wavelength. Due to its immaterial character, optical

masks are defect-free, non-destructive and species-selective.


ANF offers two main routes for applications: resist assisted neutral atom lithography (NAL) and direct deposition (DD). For NAL an atomic beam induces chemical modifications of a suitable surface which are then transferred to the underlying substrate. One of the most attractive properties of ANF is the potential to pattern neutral atom beams to directly grow nanostructures on a substrate. Direct deposition experiments have been demonstrated for sodium, chromium, aluminum, ytterbium [1] and more recently with iron [3]. The investigation of direct deposition is, however, impaired by several aspects: DD in general calls for large doses (many monolayers) in order to generate significant structural heights of a few nanometer; group III atoms, which are at the focus of this manuscript, are

known to exhibit self aggregation into nanodroplets which deform the originally deposited atomic beam pattern [4].

NAL, in contrast, offers a method to use low dosage atomic beams (few monolayers) to study the lateral distribution of atoms deposited onto substrates with nanometric resolution. The commonly used SAM resists in NAL are alkanethiols or organosilica that spontaneously form uniform monolayers on gold or silicon surfaces respectively. When a SAM is exposed to the atomic beam through a light or mechanical mask, the resist is chemically modified and wet-etching transfers the pattern into the gold or silicon substrate. The chemical process governing the neutral atom-organic monolayer interaction is very efficient but still not fully understood [5, 6].

NAL was first demonstrated with metastable argon atoms and then extended to other noble gas atoms [1]. Metastable noble gas atoms have a large internal energy (up to 20 eV for He*) that can be released on surface impact and is considered to be responsible for chemical modifications of the resist. With metastable noble gas atoms very low doses (even less than 1 atom per monolayer molecule) have been observed.

It was later found that caesium atoms [7, 8] also cause a similar chemical modification of thiol-covered gold surfaces with a threshold dosage of the order of 2 atoms per monolayer molecule. Very recently it was found that barium atoms [9] offer yet another atom-thiol surface combination applicable for neutral atom lithography. This observation has initiated us to study the interaction of Ga and In atomic beams

 Fax: +39-0832-298238, E-mail: andrea.camposeo@unile.it

*Present address: National Nanotechnology Laboratory, CNR-INFM, via Arnesano, 73100 Lecce (Italy)

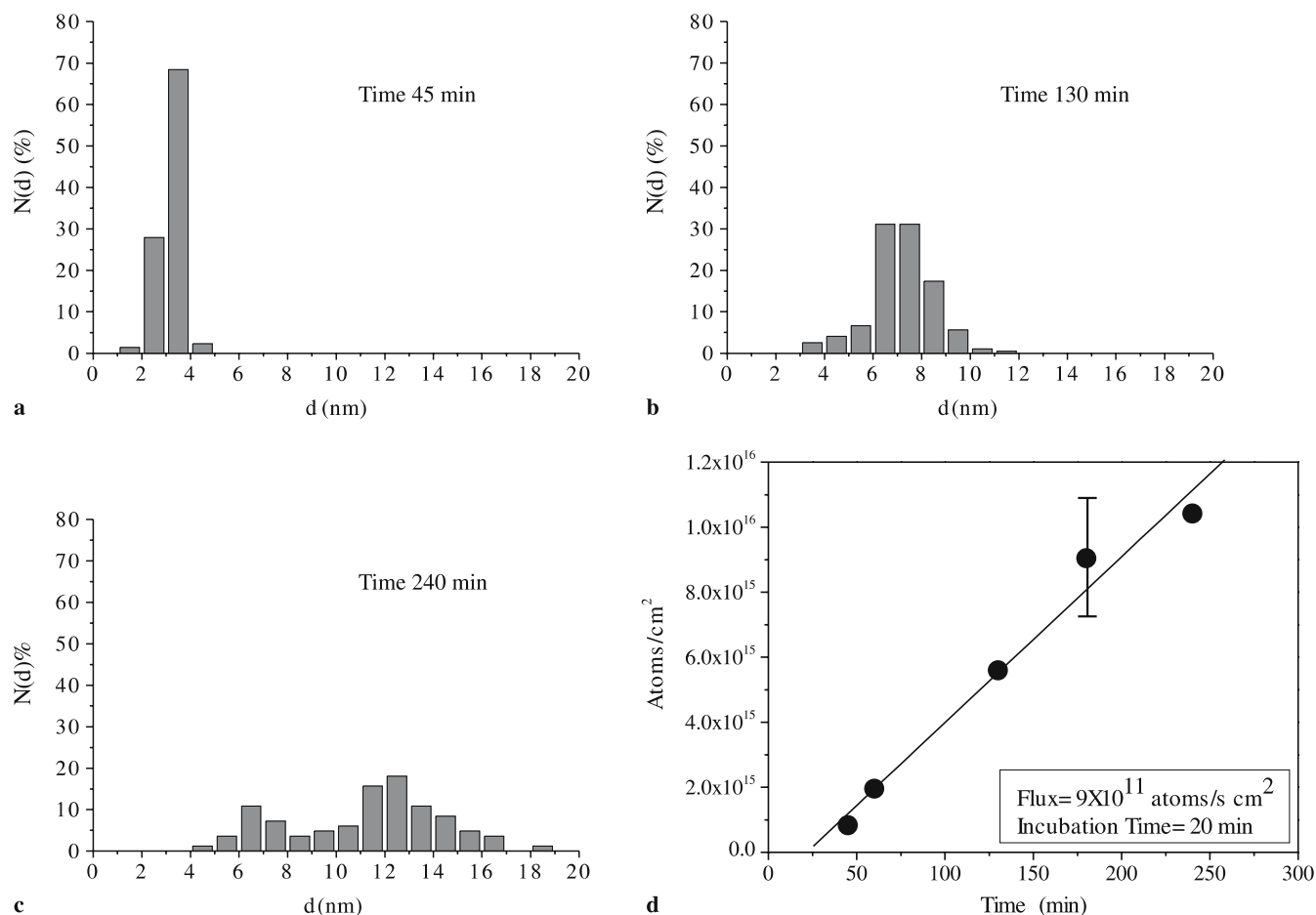


FIGURE 1 Gallium growth and deposition rate calibration. (a–c) Nanoparticle size distribution for different deposition times. A double-size distribution is evident after about 200 min due to coalescence. (d) Surface density as a function of deposition time. From a linear fit we can estimate the flux density and incubation time. The error bar on the graph includes the droplet volume and shape uncertainty of about 40%

with thiol surfaces. The potential of atom nanofabrication and laser manipulation with these technologically relevant elements is currently being studied in our laboratories [10, 11] and elsewhere [12].

In this manuscript we use gallium and indium atomic beams for resist-assisted atom lithography, showing the feasibility of the technique and estimating the threshold of the lithographic process. Our method sheds new light on the interaction of atomic beams with thiol covered gold surfaces, and it facilitates experimental investigations of the potential of group III elements for laser controlled atomic nanofabrication.

Neither the electronegativity (1.78 for In, 1.81 for Ga on the Pauling scale) nor the ionization potential (555.3 and 578.8 kJ/mol, respectively) give any clues to the different chemical interactions of In and Ga with thiol-covered surfaces used in this experiment. In our experiment, however, we find that the

threshold dose (see Sect. 4) for the modification of the substrate differs by a factor of about 4 ± 2 . The most difficult parameter in analysing these threshold doses are the atomic beam flux densities. Our experimental equipment allowed us to determine the Ga flux density with a “coalescence” method, and the In flux density with a fluorescence method. In Sect. 3 we give details of the careful analysis carried out for the calibration procedure for the two rather different methods.

2 Experimental

The two laser light sources for In and Ga have been described elsewhere [11, 13]. Here we give a brief overview of the general features of both vacuum systems. The atomic sources are VTS-Creatic effusion cells (Dual Filament) with a PBN (Pyrolytic-Boron-Nitrate) insert having a 1 mm outlet. The dual filament configuration prevents the

group III elements from condensing at the nozzle, leading to possible damaging of the oven. The effusion cell is operated at a temperature of about 1000 °C for Ga and 1200 °C for In. This provides an atomic flux of about 5×10^{15} atoms/s for gallium and 4×10^{17} atoms/s for indium calculated from the Knudsen law. For ANF we need a well collimated high flux atomic beam. A first collimation is realized geometrically by cutting the flux using an aperture with a diameter of 0.5 mm, yielding a divergence of 3 mrad for Ga and 8.8 mrad for In. The longitudinal mean velocity is of the order of 690 m/s for gallium and 560 m/s for indium. The atomic source is located inside a UHV system where ion and turbo molecular pumps maintain a background pressure below 10^{-7} Pa. The samples are placed on a holder with the surface orthogonal to the atomic beam direction.

Silicon substrates were used, covered by a sputtered 30 nm thick gold

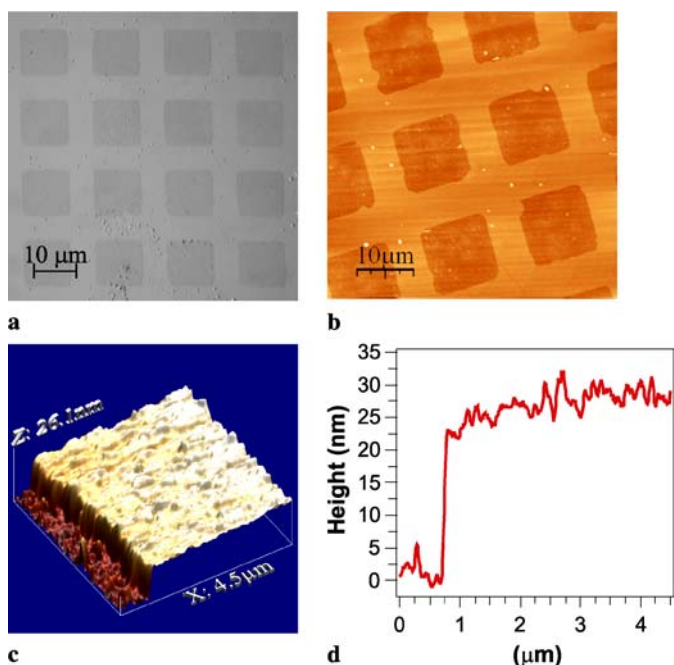


FIGURE 2 Optical and AFM images of exposed and etched gold sample with Indium (a) and Gallium (b,c). The bright regions are the ones where the gold film was not removed. The sample in (a) has been exposed for 30 min to the Indium beam with a flux of $(1.2 \pm 0.3) \times 10^{12}$ atoms/(s cm²), while the sample in (b) was exposed for 15 min to the Ga beam with a flux of $(9 \pm 4) \times 10^{11}$ atoms/(s cm²). (c) is a close-up of a step from the sample in (b). (d) Line profile of the step reported in figure (c). From the rising edge we can extrapolate the minimal resolution of 80–90 nm

layer, with an adhesion layer (5 nm thick) of chromium. The monolayer of nonanethiole molecules ($\text{CH}_3(\text{CH}_2)_8\text{SH}$) forms on top of the gold substrate by dipping into a 2–5 mM ethanol solution for 24 h. Before SAM growth, the gold substrates were cleaned with piranha solution. In order to pattern the substrate with the Ga and In atoms, different physical masks can be mounted close to the SAM layer. We will specifically present results obtained using nickel mesh with orthogonal periods 16.5 μm and 16.9 μm, and with 11.5 μm and 9.9 μm square openings respectively. After exposure to Ga and In beams (typically 15 min for Ga and 30 min for In) the samples are removed from the vacuum chamber and immersed in a wet chemical etching solution [14] that removes the gold layer in the region where there is no more protection by the pristine SAM. The optimal etching time is about 10 min, as explored by calibration measurements of the etching rate.

3 Flux estimates

The Ga flux density was estimated by analysing the growth of

Ga nanoparticles on Si(100) surfaces at room temperature [4]. The gallium nano-droplets grow in the Volmer-Weber mode [15, 16] i.e. under partial wetting conditions. We performed transmission electron microscopy (TEM) analysis of the deposited samples using a JEOL JEM-2010 field emission TEM operating at 200 kV. By TEM analysis it was possible to characterize the cluster size distribution for different deposition times (Fig. 1a-c).

The cluster size increases with the deposition time as expected, and after about 200 min a double-size distribution is evident. From the size distribution we can estimate the volume of the droplets assuming a semi-spherical shape and knowing the gallium density of 6.095 g/cm³ [17]. Using the known sticking coefficient of gallium on silicon which is unity [18], we calculate the number of atoms deposited over an area as large as the TEM image. Hence we can analyze the surface density temporal evolution as shown in Fig. 1d. The linear fit of these data gives a flux density of $(9 \pm 4) \times 10^{11}$ atoms/(s cm²) in the deposition region. The 40% uncertainty of the flux value takes into account the uncertainty of the droplet volume and

shape. As an aside we get the incubation time [19] of about 20 min, this is the time needed for Ga atoms to coalesce into larger structures.

The indium atomic beam flux density was determined by recording the spatially resolved fluorescence intensity of the laser excited atomic beam with a calibrated photodiode and a CCD camera. Indium has a $P_{1/2,3/2}$ doublet ground state connected by 410 nm and 451 nm transitions to the first excited state [13]. Due to the 2 : 3 branching ratio for the decay into the $P_{1/2}$ and $P_{3/2}$ states, fluorescence induced by excitation with a single laser line at 410 nm rapidly terminates. At intensities well above the saturation value of $I_{\text{sat}} = 16.9$ mW/cm² every indium atom scatters 1.32 photons, leaving the fluorescence intensity directly proportional to the atomic beam density. We have experimentally checked that for the used laser intensity at 410 nm the In atoms are indeed driven into the saturation limit. The atomic beam fluorescence was collected from an effective solid angle of $4\pi/20$ which was measured by aperturing the imaging lens.

The exposure of substrates for the determination of the threshold dose was carried out at the same position as the fluorescence measurement, thus reliable experimental data for the spatial flux density distribution at the substrate were available. The center flux density used in the experiment to determine the threshold dose in Sect. 4 was $(9 \pm 2) \times 10^{12}$ atoms/(s cm²).

4 Results and discussion

The gold samples were exposed to the atomic beams for 5–30 min and wet etched for 10 min. The patterned gold samples were then analyzed by both optical microscopes and atomic force microscopes (AFM). Figure 2a shows a typical optical microscope image of a patterned gold sample exposed to the In beam through a 16.9 μm period mask, while Fig. 2b shows an AFM image of a sample exposed to the Ga beam through a 16.5 μm period nickel mask. The presence of a well defined structure shows that gallium and indium atoms chemically modify the nonanethiol molecules of the SAM layer covering the substrates. The pattern of the masks is well transferred to the gold

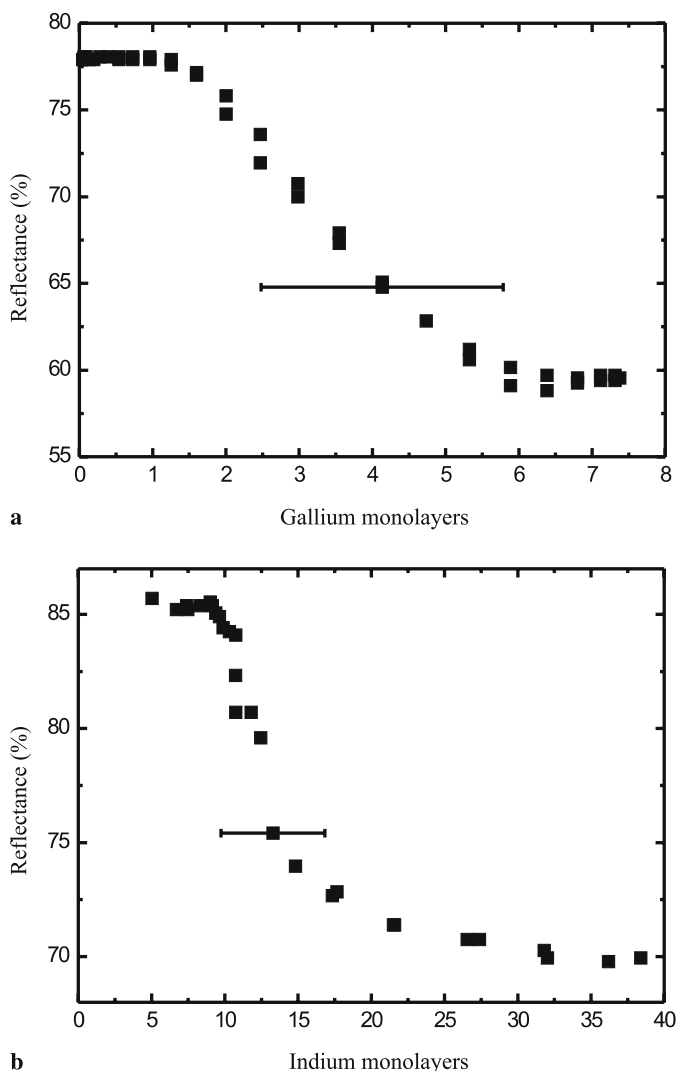


FIGURE 3 Reflectance of an etched gold surface after exposure and etching as a function of the dose of Ga atoms, top plot, and of In atoms, bottom plot. For In the reflectance is already maximized at 10 monolayers and remains at that level even below 5 monolayers where no data are marked. A monolayer is defined to have the surface density of the SAM (4.6×10^{14} atoms/cm²). Representative error bars dominated by the uncertainty in the flux density calibration are given

layer. The AFM image Fig. 2c shows sharp edges of about 80 nm (Fig. 2d) calculated from the 10 to 90% of the total height. The edge resolution is mainly limited by the grain size of the gold film, of the order of 100 nm [5]. This resolution can be improved in principle by using anisotropic etching solutions, thiol molecules with a shorter alkyl chain and surfaces sustaining more homogeneous SAM layers [5].

Resist-assisted atom lithography is characterised by the presence of a threshold dose [8]. We have measured this threshold for Ga/In using the technique reported in [8], based on reflectance measurements of an etched gold sample. The substrates were exposed to the atomic beam without using

a mask. The local dose however varies as a consequence of the profile of the atomic beam. After removal from the vacuum chamber the reflectivity profile of the etched samples was measured with laser light (632 nm) at normal incidence. Using the known flux profile of the atomic beam and the measured reflectivity profile of the exposed region, the damage of the surface can be determined as a function of the local Ga/In dose. The results are shown in Fig. 3. The data show the threshold of the lithographic process which we define to be the dose at which the reflectance change has reached half the value obtained at large doses. It is of order 3 ± 1 monolayers for gallium and 12 ± 3 monolayers for indium.

The process responsible for the SAM damage i.e. for the molecule modification after the interaction with neutral atoms, either alkalis or group III atoms, is still not well understood, as discussed in [9]. The energies of ground state atoms in an atomic beam are of the order of few tens of meV, well below the typical binding energy of the thiol molecule to the gold surface. For ground state atoms chemical interaction should be responsible for the molecule damage. A possible explanation is that Ga and In atoms travel to the bottom of the SAM layer, through its open defects, and interact with the sulfur-gold bond. This explanation is supported by the observation that the long range order of the SAM layer plays a role for structural resolution obtained with this methods [5, 7], and that regions exposed to the atomic beam exhibit afterwards an increased degree of disorder [20]. Also the formation of ionic species Ga⁺ and In⁺ cannot be excluded, as a consequence of the interaction between the Ga and In atoms and the Au surface and an interaction of the ionic species with the thiol molecule, as recently suggested for the caesium case [6]. Indeed further investigations are needed to clarify the chemical-physical SAM-neutral atom interaction, for all atomic species applied so far.

5 Conclusions

In conclusion we have demonstrated that neutral gallium and indium beams chemically modify thiol monolayers adsorbed on a gold surface with nanometric resolution, thus establishing two new systems for resist assisted neutral atom lithography. We have shown that the sensitivity of the new combinations is compatible with known systems. Experimental analysis of laser controlled deposition of Ga and In on substrates is facilitated since small doses are only required. Further investigation of the Ga/In-SAM systems may also shed new light on the mechanism of the atom-thiol layer interaction which is still not well understood.

ACKNOWLEDGEMENTS We are grateful to S. Spadaro and S. Patané for the AFM images and to C. Bongiorno and C. Spinella for TEM analysis. This work was supported by the FIRB Project of the MIUR with “Manipolazione su scala nanometrica attraverso tecnologie di raffreddamento laser” and by the

NANOCOLD project of the IST programme of the EU through the Nanotechnology Information Devices Initiative.

REFERENCES

- 1 D. Meschede, H. Metcalf, *J. Phys. D Appl. Phys.* **36**, R17 (2003)
- 2 M.K. Oberthaler, T. Pfau, *J. Phys. Condens. Matter* **15**, R233 (2003)
- 3 E. te Sligte, B. Smeets, K.M.R. van der Stam, R.W. Herfst, P. van der Straten, H.C.W. Beijerinck, K.A.H. van Leeuwen, *Appl. Phys. Lett.* **85**, 4493 (2004)
- 4 B. Fazio, O.M. Maragò, E. Arimondo, C. Spinella, C. Bongiorno, G. D'Arrigo, *Superlattices Microstruct.* **36**, 219 (2004)
- 5 C. O'Dwyer, G. Gay, B. Viaris de Lesegno, J. Weiner, *Langmuir* **20**, 8172 (2004)
- 6 C. Di Valentin, A. Scagnelli, G. Pacchioni, *J. Phys. Chem. B* **109**, 1815 (2005)
- 7 M. Kreis, F. Lison, D. Haubrich, D. Meschede, S. Nowak, T. Pfau, J. Mlynek, *Appl. Phys. B* **63**, 649 (1996)
- 8 K.K. Berggren, R. Younkin, E. Cheung, M. Prentiss, A.J. Black, G.M. Whitesides, D.C. Ralph, C.T. Black, M. Tinkham, *Adv. Mater.* **9**, 52 (1997)
- 9 A. Camposeo, A. Fioretti, F. Tantussi, S. Gozzini, E. Arimondo, C. Gabbanini, *Appl. Phys. B* **79**, 539 (2004)
- 10 H. Leinen, D. Glässner, H. Metcalf, R. Wynands, D. Haubrich, D. Meschede, *Appl. Phys. B* **70**, 567 (2000)
- 11 O.M. Maragò, B. Fazio, P.G. Gucciardi, E. Arimondo, *Appl. Phys. B* **77**, 809 (2003)
- 12 S.J. Rehse, K.M. Bockel, S.A. Lee, *Phys. Rev. A* **69**, 063404 (2004)
- 13 U. Rasbach, J. Wang, R. dela Torre, V. Leung, B. Klöter, D. Meschede, T. Varzhapetyan, D. Sarkisyan, *Phys. Rev. A* **70**, 033810 (2004)
- 14 Y. Xia, X.Z. Zhao, E. Kim, G.M. Whitesides, *Chem. Mater.* **7**, 2332 (1995)
- 15 E. Sondergard, R. Kofman, P. Cheyssac, A. Stella, *Surf. Sci.* **364**, 467 (1996)
- 16 M. Zinke-Allmang, L.C. Feldman, W. van Saarloos, *Phys. Rev. Lett.* **68**, 2358 (1992)
- 17 W.H. Hoather, *Proc. Phys. Soc.* **48**, 699 (1936)
- 18 K. Carleton, S.R. Leone, *J. Vac. Sci. Technol. B* **5**, 1141 (1987)
- 19 C. Spinella, S. Lombardo, F. Priolo, *J. Appl. Phys.* **84**, 5383 (1998)
- 20 M.L. Chabinyc, J.C. Love, J.H. Thywissen, F. Cervelli, M.C. Prentiss, G.M. Whitesides, *Langmuir* **19**, 2201 (2003)